Journal of Catalysis **200,** 91–98 (2001)
doi:10.1006/jcat.2001.3183, available online at http://www.idealibrary.com on IDEAL®

Kinetics of Vanadyl Etioporphyrin Hydrodemetallization

Fei Xiang Long and Börje S. Gevert[1]

Department of Applied Surface Chemistry, Chalmers University of Technology, 412 96 Göteborg, Sweden

Received September 26, 2000; revised January 12, 2001; accepted January 15, 2001; published online April 11, 2001

The kinetics of hydrodemetallization (HDM) of vanadyl etioporphyrin (VO-EP) has been studied in a batch autoclave at 543 K and 5 MPa of total pressure, with white oil as solvent and presulfiding $CoMo/Al_2O_3$ (TK 710) as catalyst. The most widely accepted kinetic model comprised of only dihydrogenated intermediate (VO-EPH_2) does not fit our experimental data. A new model with two reversible hydrogenation steps and a lumped irreversible hydrogenolysis step is proposed, and follows the concentration trace of reactants (VO-EP and VO-EPH_2) very well for most reaction times. The different modeling stems from the different selectivity of the catalysts. Under our experimental conditions the slowest step is the terminal hydrogenolysis instead of the first hydrogenation, so the steps after the first hydrogenation cannot be lumped into one step in modeling our experimental data. Thus, the whole kinetic scheme should incorporate the tetrahydrogenated species (VO-EPH_4) found in our samples.

Key Words: **porphyrin; metal porphyrin; vanadyl porphyrin; etioporphyrin; kinetics; hydroprocessing; hydrotreating; hydrodemetallization; HDM; CoMo catalyst.**

INTRODUCTION

Hydrodemetallization (HDM) is a pretreatment process in resid hydrodesulfurization (RDS) that is designed to upgrade residua so that the products could be efficiently processed in downstream conversion units (coking, catalytic cracking, hydrocracking, etc.). The HDM unit is used to eliminate metal contaminants from streams to protect downstream catalysts in RDS. The most abundant and problematic metals in residua are vanadium and nickel that will deposit on a HDM catalyst surface as metal sulfides. The gradual buildup of these metal deposits poisons active sites, blocks pores, and ultimately determines the operating lifetime of the catalyst (1). Thus, a better understanding of kinetics concerning HDM of metallic petroleum constituents is very important to improving and developing HDM catalysts and reactors.

Nevertheless, because of the numerous types of heteroatoms naturally occurring in crudes with unspecified nature and quantity, investigating HDM kinetics is often performed with model compounds. The use of model compounds provides insight into fundamental rate processes that occur, and shows the behavior of real feedstocks in commercial HDM reactors. Three kinds of vanadium or nickel porphyrins have been frequently used as model compounds in HDM studies: metal etioporphyrins (Etio type), metal tetraphenylporphyrins (TPP type), and metal tetra(3-methylphenyl)porphyrins (T3MPP type) (2–19). Etio-type metalloporphyrins in addition to DPEP-type (deoxophylloerythroetioporphyrin) have been identified in crude oils as the principal groups that the majority of metalloporphyrins fall into, and etioporphyrins comprise up to 50% of the metal in the free porphyrin fraction (20). Considering that vanadium is the most abundant metal in most crudes and metal etioporphyrins naturally occur in petroleum rather than synthetic chemicals, vanadyl etioporphyrin (VO-EP) is definitely representative of the model compounds and thereby is chosen in this HDM study.

Wei and co-workers (2–7) conducted pioneering and remarkable HDM kinetic studies with model compounds. Complementary work was done by Rankel and Rollmann (8, 9), Kameyama *et al.* (10–12), Weitkamp *et al.* (13, 14), Gerhardt (15), Morales *et al.* (16), Chen and Massoth (17), and Moulijn and co-workers (18, 19). As for VO-EP the previous studies are summarized as follows. Hung and Wei obtained fractional order kinetics centered on 0.5 for up to 90% vanadium removal (2). Agrawal and Wei proposed a sequential HDM mechanism to VO-EP comprised of a reversible hydrogenation step and a lumped irreversible hydrogenolysis step (3). Smith and Wei (7) and Morales *et al.* (16) confirmed the consecutive mechanism, but Morales *et al.* concluded that the direct demetallization of initial porphyrin by thermal cleavage could not be ruled out. The limited results indicate that the exact HDM kinetics of VO-EP still remains unclear in literature. The objective of this study is to investigate the intrinsic HDM kinetics of vanadyl etioporphyrin over a sulfided $CoMo/Al_2O_3$ catalyst in a batch stirred autoclave.

EXPERIMENTAL METHODS

The feed of this HDM kinetic study consisted of vanadyl(IV)-etioporphyrin-I (VO-EP) (Fig. 1a) and white

[1] To whom correspondence should be addressed. Fax: (46 31) 160062. E-mail: gevert@surfchem.chalmers.se.

0021-9517/01 $35.00

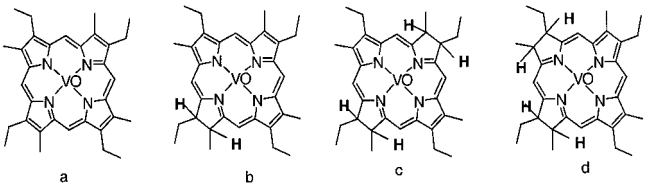

FIG. 1. Molecular structures of vanadyl etioporphyrin (VO-EP) and its hydrogenated species: (a) vanadyl etioporphyrin (VO-EP), (b) vanadyl etiochlorin (VO-EPH$_2$), (c) vanadyl etiobacteriochlorin (VO-EPH$_4$), and (d) vanadyl etioisobacteriochlorin (VO-EPH$_4$).

oil. The method of dissolving VO-EP purchased from Midcentury Chemicals (Posen, IL) into the white oil (Primol 352) from Exxon was based on the description by Hung and Wei (2). Commercial $CoMo/Al_2O_3$ hydroprocessing catalyst TK 710 (Haldor Topsoe AS) received as 1/32-in. extrudates was crushed to 0.074–0.088 mm (200–170 mesh), which was reported the absence of diffusional effects (2), to investigate the intrinsic kinetics. Presulfiding the catalyst, which was achieved in an independent microreactor with a mixture of 10 vol% hydrogen sulfide in hydrogen at 673 K for 2 h, was chosen to represent industrial working conditions. All the runs were performed in a 300 cm^3 stirred autoclave described in detail in an earlier publication (21). Subsequent modifications of the reactor included additions of a catalyst loader and a sampling line with a porous metal filter. The catalyst loader made of a $\frac{1}{2}$-in. o.d. tube with two $\frac{1}{4}$-in. ball valves at both ends was used to inject catalysts into the autoclave when the desired reaction temperature was reached to avoid HDM reactions during the heating period. The sintered stainless steel filter with 0.5 μm pore diameter prevented loss of the catalyst when liquid samples were taken.

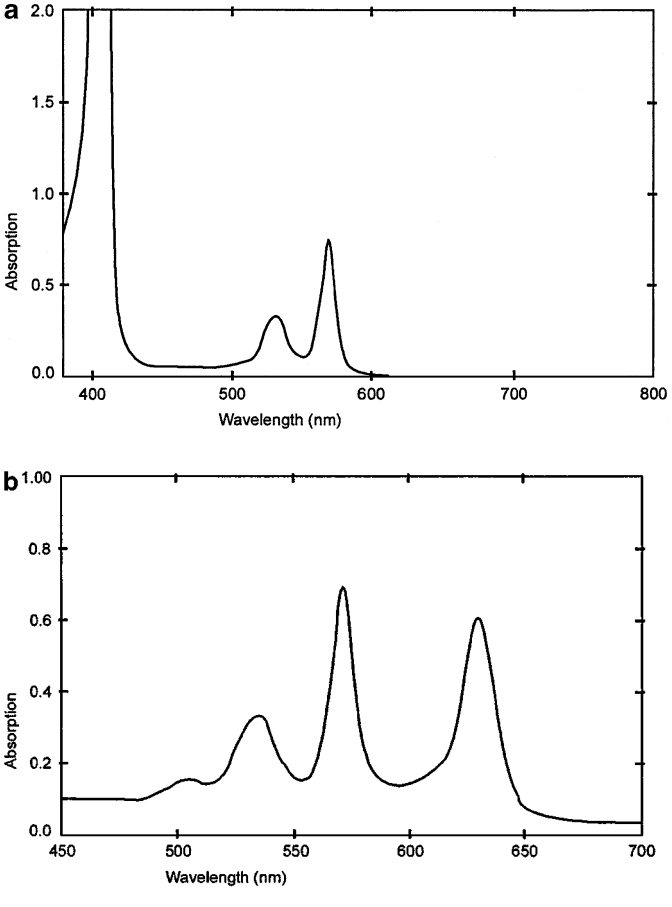

FIG. 2. Spectra of (a) vanadyl etioporphyrin and (b) the liquid sample taken from HDM experiments on vanadyl etioporphyrin.

An ultraviolet–visible spectrophotometer was routinely employed to determine the concentrations of the porphyrinic reactant as well as the reaction intermediates in the liquid samples that were diluted by xylene first. Vanadyl etioporphyrin was red in color and had intense absorption peaks in the visible band as shown in Fig. 2a. The typical spectrum of the samples is given in Fig. 2b in which the intensive new peak at 631 nm was caused by the porphyrinic intermediate: vanadyl etiochlorin (VO-EPH$_2$, Fig. 1b) (3). Moreover, other minor peaks around 505 nm (Fig. 2b) and 770 nm were also detected by using the peak-pick function of the spectrophotometer. The absorption at 505 nm was significant while the one at 770 nm was very weak in comparison with the characteristic absorptions of VO-EP at 571.5 nm and VO-EPH$_2$ at 631 nm. In analogy with literature (22), the peaks at 505 nm and 770 nm were assigned to tetrahydrogenated species (VO-EPH$_4$): vanadyl etioisobacteriochlorin and vanadyl etiobacteriochlorin (Figs. 1c, 1d). Calibration factors were 0.56 Abs/ppm V for VO-EP (571.5 nm), and 0.61 Abs/ppm V for vanadyl etiochlorin (VO-EPH$_2$, 631 nm) (3). Unfortunately, the extinction coefficients of vanadyl tetrahydrogenated species were not found in the literature, so the absolute concentrations of the species were not determined.

Kinetic parameters were estimated by the least-squares method. In order to account for the effect of decreasing reactant volume due to sampling, a corrected space-time was used (21). The coupled differential equations were solved numerically by using the solver "ode15s" in commercial software MATLAB 5.3. The objective function, defined as the sum of squares of the differences between the experimentally observed values and the values calculated from the regression equation, was minimized by the solver "lsqnonlin" set to "Trust-region Reflective Newton" algorithm.

A summary of the experimental runs is provided in Table 1.

RESULTS AND DISCUSSION

1. Noncatalytic Demetallization Reactions and Transient Period

Five runs (VF1, VF2, VF4, VF18, and VF19) were performed without catalysts to investigate the effects of thermal dissociation of VO-EP. The concentration changes of

TABLE 1

Experimental Runs

Run no.	Temp. (K)	Total pressure (MPa)	Reactant wt. (g)	Cat. wt. (g)	Oil/cat.	Zero reaction time concn (ppm)[a]	Duration of reaction (h)	Using cat. loader
VF1	603	5(N_2)	125.989	0		7.916	19.5	No
VF2	603	6(N_2)	87.385	0		25.481	21.33	No
VF4	543	5	80.130	0		8.584	23.25	No
VF5	543	5	100.516	0.156	644.333	8.700	9	Yes
VF6	543	5	170.304	0.292	583.233	9.151	7	Yes
VF8	543	5	170.172	0.668	254.749	8.560	6.5	Yes
VF10	543	5	170.753	0.6	284.588	8.791	4.75	Yes
VF12	543	5	170.865	1.093	156.327	22.364	10	Yes
VF13	543	5	171.110	1.049	163.117	24.360	8.5	Yes
VF14	543	5	174.109	1.055	165.032	15.496	8.08	Yes
VF15	543	5	172.117	0.476	361.590	27.667	50.5	Yes
VF16	543	5	171.952	0.479	358.981	19.856	30.5	Yes
VF18	543	7(N_2)	102.638	0		25.334	68.25	No
VF19	543	7(N_2)	102.317	0		18.911	115.59	No
VF20	543	7	101.445	0.165	613.331	7.233	15.25	No
VF21	543	7	100.288	0.167	600.887	14.005	66	No
VF22	543	7	101.395	0.334	303.396	9.935	10.58	No
VF24	543	7	102.037	0.237	430.536	34.113	168	Yes

[a] The sum of vanadium concentrations in VO-EP and VO-EPH_2 at zero reaction time.

VO-EP were statistically insignificant in all five runs, and no hydrogenated intermediates were detected even under hydrogen (VF4). Three runs (VF20, VF21, and VF22) were operated differently: the feed and catalyst were heated together under nitrogen first. After 1.4 h (VF20), 3 h (VF21), and 3 h (VF22), the reactant color did not change noticeably, indicating that no obvious demetallization reactions happened. However, just less than 1 min after nitrogen was replaced by hydrogen, the samples taken had changed color accompanied by production of a significant amount of hydrogenated intermediates (VO-EPH_2). Therefore, hydrogen, catalyst, and a suitable temperature were concluded to be the necessary factors for demetallization of VO-EP under our experimental conditions.

A transient period, characterized by an extremely quick drop of the VO-EP concentration while the catalyst was introduced into the reactor, was observed in all HDM runs. The initial reduction of VO-EP concentration was found proportional to catalyst weight or oil (g)/catalyst (g) with limited records (Fig. 3). The unit drop calculated from the data was 16.916 ppm/g cat. This transient period was explained by the strong adsorption of VO-EP on the catalyst: physical adsorption on catalyst carriers, and chemical adsorption on active sites of the catalyst. In fact, alumina is such a well-known adsorbent for separation of porphyrinic species in the laboratory by "dry column" chromatography (3, 23). Furthermore, because the solution color changed from red to red purple as soon as the catalyst had contacted the reactant, the adsorption and desorption were thought to be very fast. To explore the intrinsic HDM kinetics, only the data obtained after this transient period were considered. Zero reaction time was referred to the moment when the first sample was drawn, which was 1–2 min after the catalyst was pressed into the autoclave by hydrogen. It was thought that the further decline of VO-EP concentration was controlled by the intrinsic HDM kinetics.

2. Catalytic Demetallization Reactions

2.1. Reaction mechanism. The representative concentrations or absorption versus space-time curves are shown in Fig. 4: VO-EP and VO-EPH_2 were expressed in absolute

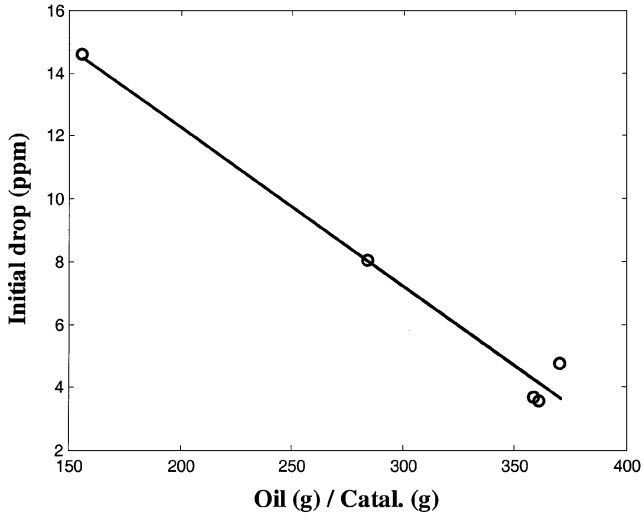

FIG. 3. Relationship between the initial drop of VO-EP and oil/catalyst. The data are from VF10, 11, 12, 15, and 16.

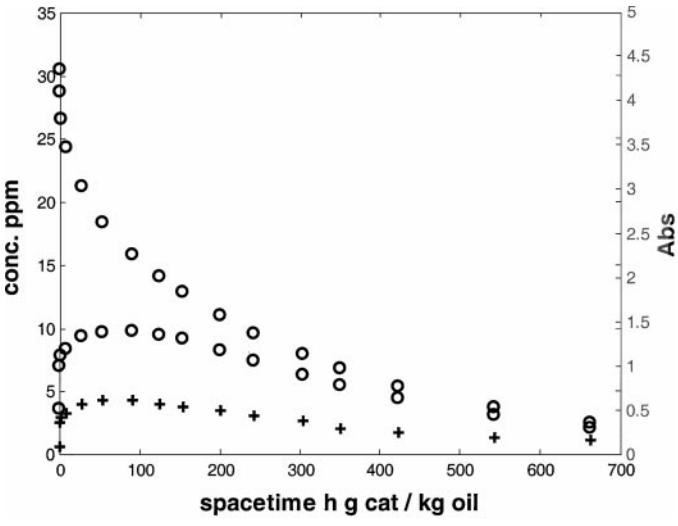

FIG. 4. Representative concentrations or absorption versus spacetime curves from the HDM experiments in the example of VF24. Symbols: (○) concentration of VO-EP and VO-EPH$_2$; (+) absorption of VO-EPH$_4$. Conditions: 7 MPa, 543 K.

concentration (ppm), and VO-EPH$_4$ was expressed in absorption units corrected for overlap at 505 nm with absorption bands of other porphyrinic compounds. The rise and then fall of VO-EPH$_2$ and VO-EPH$_4$ were characteristic; substance VO-EPH$_2$ and VO-EPH$_4$ were intermediates in the overall reaction in which VO-EP was transformed into its products. This observation was in good agreement with the chemistry of metalloporphyrins: under the chemical reduction condition metalloporphyrins can be successively reduced several times until the macrocycle of the porphyrin is broken, losing the character of porphyrin (24). It was also consistent with the previous studies: under similar reaction conditions (hydrogen and CoMo/Al_2O_3 catalyst), Ni-TPP and Ni-T3MPP favored being successively and reversibly hydrogenated twice at β-pyrrolic positions to tetrahydrogenation species with isobacteriochlorin dominating (4, 18). As for etio-type metalloporphyrins, although the dihydrogenated species were found to be the dominating intermediate in some cases, higher hydrogenated products were possible. Agrawal and Wei reported that the intermediate of metal etioporphyrins HDM reactions could be further separated into the yellowish green group and the bluish green group (3). This implied that apart from the dihydrogenated other hydrogenated species existed in the intermediate. On the basis of the analysis above, the HDM reaction mechanism of VO-EP was deduced as follows. Under hydrogen pressure and hydroprocessing catalysts, VO-EP favors being successively and reversibly dihydrogenated twice at β-pyrrolic positions to tetrahydrogenation species, and then ends in a hydrogenolysis step: the breaking of the porphyrin macrocycle and the deposit of the metal on the catalyst. Higher hydrogenated species are possible, but their quantity is too small to be detected.

2.2. Reaction modeling. Kinetic models can be proposed on the basis of the known HDM reaction mechanism of VO-EP. Nevertheless, macroscopic kinetic study is characterized by assumptions of quasi-equilibrium and rate-determining steps to avoid too many parameters that must be empirically adjusted. That means not all elementary steps in the reaction mechanism appear in kinetic models; only those steps whose rates are significantly slower than those of the other steps with which they are coupled will be involved in kinetic models.

2.2.1. Fitting the experimental data with the most accepted kinetic model. Model 1 with a reversible hydrogenation step and a lumped irreversible hydrogenolysis step (Fig. 5a) is accepted most widely for the HDM reactions of VP-EP by now. This model, initiated by Agrawal and Wei (3), did not include the tetrahydrogenation species, because under their experimental conditions the slowest step in the kinetic scheme was the first hydrogenation. VO-EPH$_2$ was regarded as going through very quick successive hydrogenation reactions and ending in the last hydrogenolysis step. In kinetic modeling, these fast steps were treated as a lumped irreversible hydrogenolysis step. The typical fitting results of our experimental data to Model 1 in the examples of VF8 and 16 are shown in Fig. 6. Unfortunately, obvious deviations from the trace of VO-EP and VO-EPH$_2$ were observed for all HDM runs.

The failure of Model 1 was explained by the fact that the first hydrogenation was no longer the slowest step in the whole kinetic scheme under our experimental conditions. For all HDM runs, VO-EPH$_2$ reached its maximum

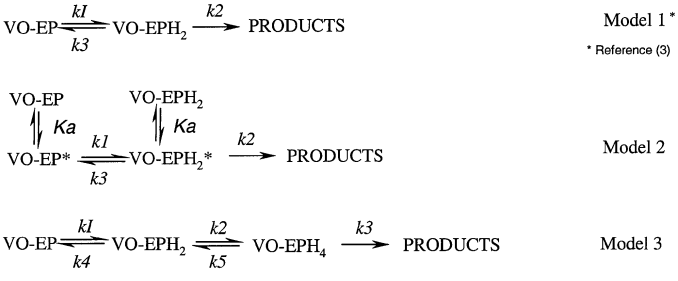

a

$$r_{VO\text{-}EP} = -k1\, C_{VO\text{-}EP} + k4\, C_{VO\text{-}EPH_2} \quad (1)$$

$$r_{VO\text{-}EPH_2} = k1\, C_{VO\text{-}EP} - (k2+k4)\, C_{VO\text{-}EPH_2} + k5\, C_{VO\text{-}EPH_4} \quad (2)$$

$$r_{VO\text{-}EPH_4} = k2\, C_{VO\text{-}EPH_2} - (k3+k5)\, C_{VO\text{-}EPH_4} \quad (3)$$

b

FIG. 5. (a) Kinetic models proposed for HDM reactions of VO-EP. All steps (k_1–k_3) in the models were assumed to be first order in metal concentrations while K_a was the adsorption coefficient. VO-EP* and VO-EPH$_2^*$ referred to the adsorbed species, and products referred to metal deposits on the catalyst and ring fragments of VO-EP. (b) Rate expressions of Model 3.

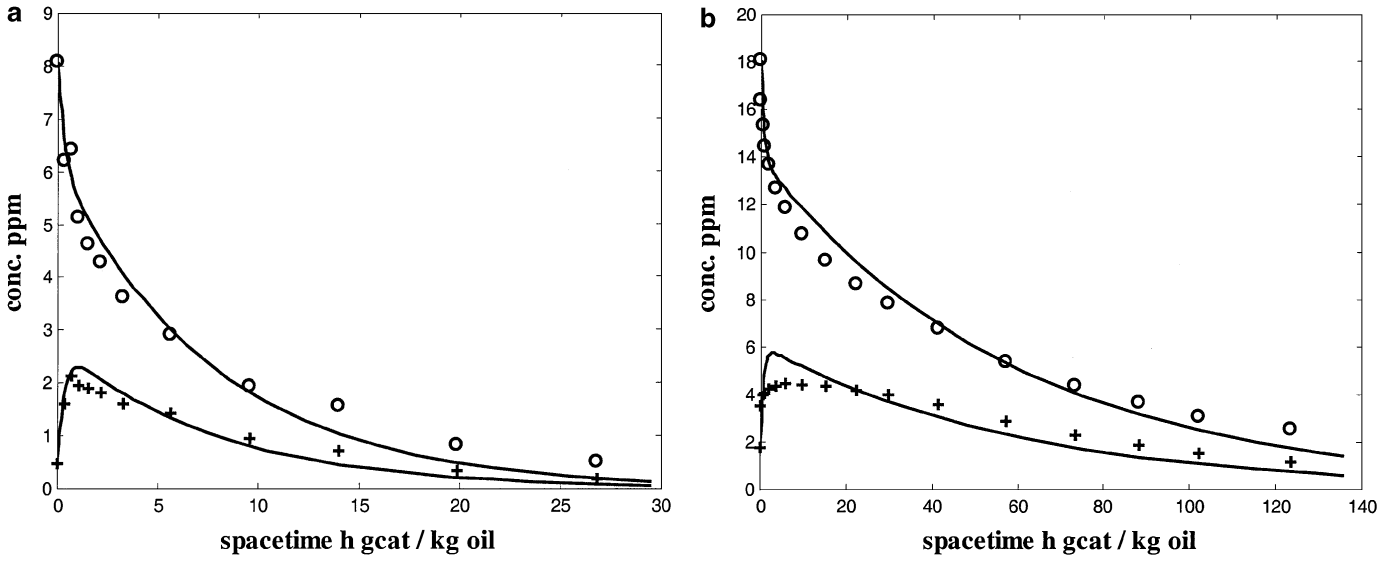

FIG. 6. Typical experimental and modeling results of VO-EP HDM for Model 1 with VF8 (a) and VF16 (b). Solid lines represent the modeling results. Symbols: (○) concentration of VO-EP; (+) concentration of VO-EPH$_2$. Conditions: 5 MPa, 543 K.

extremely fast (usually within 1 h) as shown in Fig. 6. After that VO-EP and VO-EPH$_2$ were in a pseudoequilibrium state: decaying in the same very small reaction rate as indicated at the late stage of the logarithmic plot of VO-EP and VO-EPH$_2$ in Fig. 7. All regression results with Model 1 showed that the slowest step in the overall demetallization scheme was the last hydrogenolysis under our experimental conditions, rather than the hydrogenation step in any others' (3, 4, 7, 18). Therefore, the second hydrogenation step (from VO-EPH$_2$ to VO-EPH$_4$) and the last hydrogenolysis step lost the justice of being treated as a lumped step in modeling our experimental data. The different rate-limiting steps were a result of the different selectivity of the catalysts. The selectivity of the catalyst, defined as the terminal hydrogenolysis step rate constant divided by the initial hydrogenation step rate constant, was below

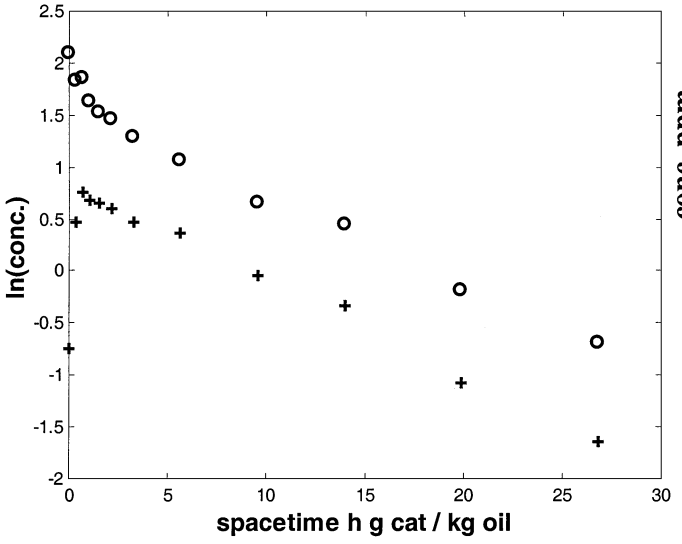

FIG. 7. Logarithmic plot of VO-EP and VO-EPH$_2$ concentrations versus space-time with VF8. Symbols: (○) VO-EP; (+) VO-EPH$_2$. Conditions: 5 MPa, 543 K.

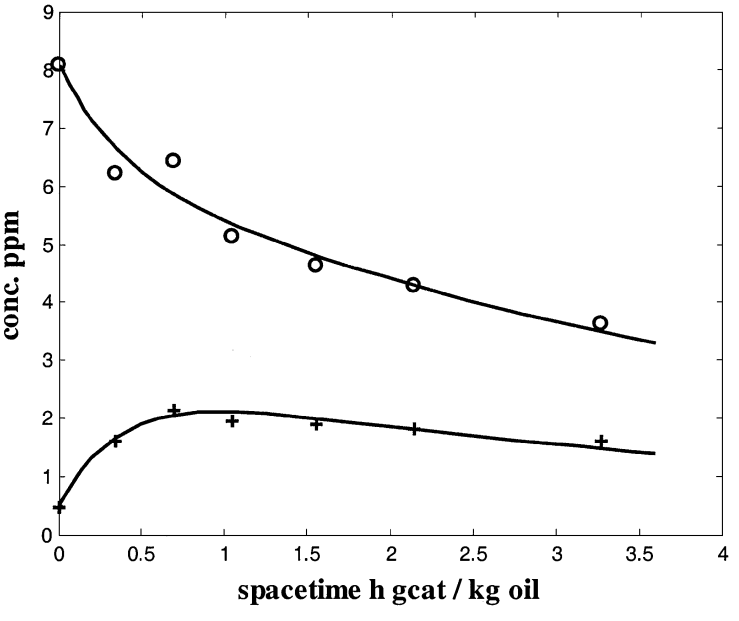

FIG. 8. Typical experimental and modeling results of VO-EP HDM for Model 1 with VF8: only the data from the beginning of the reactions are used. Solid lines represent the modeling results. Symbols: (○) concentration of VO-EP; (+) concentration of VO-EPH$_2$. Conditions: 5 MPa, 543 K.

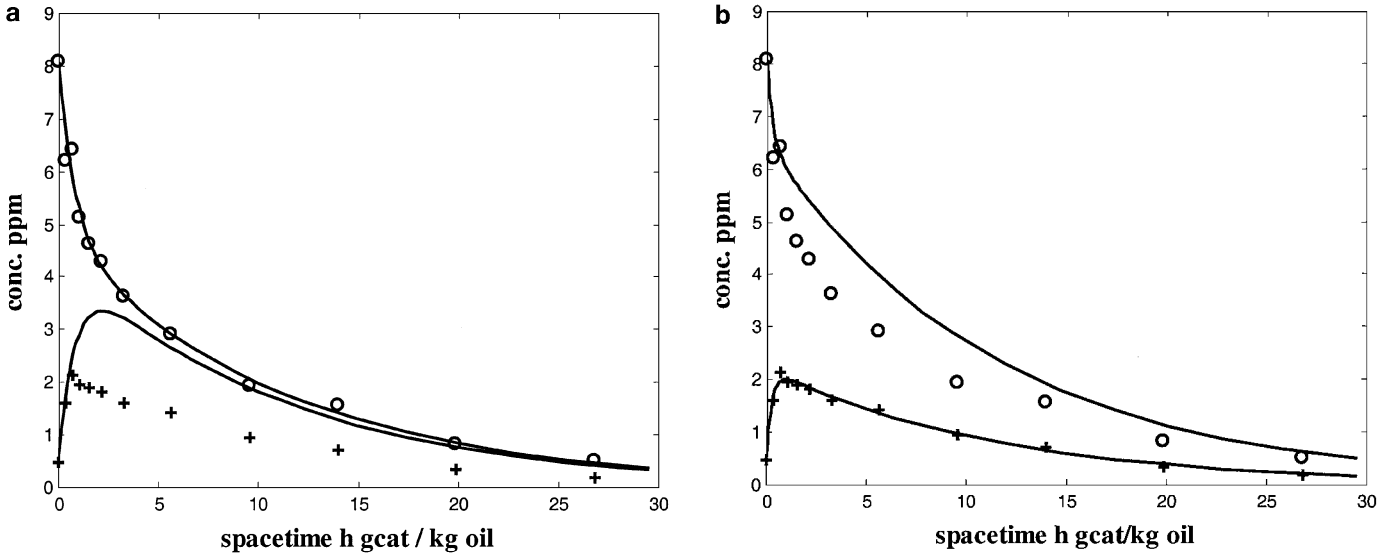

FIG. 9. Typical experimental and modeling results of VO-EP HDM for Model 1 with VF8: (a) only the data of VO-EP are used; (b) only the data of VO-EPH_2 are used. Solid lines represent the modeling results. Symbols: (○) concentration of VO-EP; (+) concentration of VO-EPH_2. Conditions: 5 MPA, 543 K.

1 (mostly around 0.1) in our experiments, in contrast to 1.4 in Smith's experiments (7). This meant our catalyst had a higher hydrogenation ability than that of hydrogenolysis.

Nevertheless, although Model 1 did not fit the full time course of VO-EP and VO-EPH_2 well, interestingly it fit the beginning period data of both VO-EP and VO-EPH_2 very well (Fig. 8 illustrated with VF8). Moreover, Model 1 followed the full time course of either VO-EP or VO-EPH_2 very well, if the single data set of VO-EP or VO-EPH_2 was used in fitting at one time (Figs. 9a and 9b illustrated with VF8).

In addition, Model 2, a Langmuir–Hinshewood–Hougen–Watson (LHHW) form of Model 1 (Fig. 5a), was examined as well. Although there were more adjusted parameters than Model 1 the fitting was hardly improved, indicating that the addition of an inhibition term could not

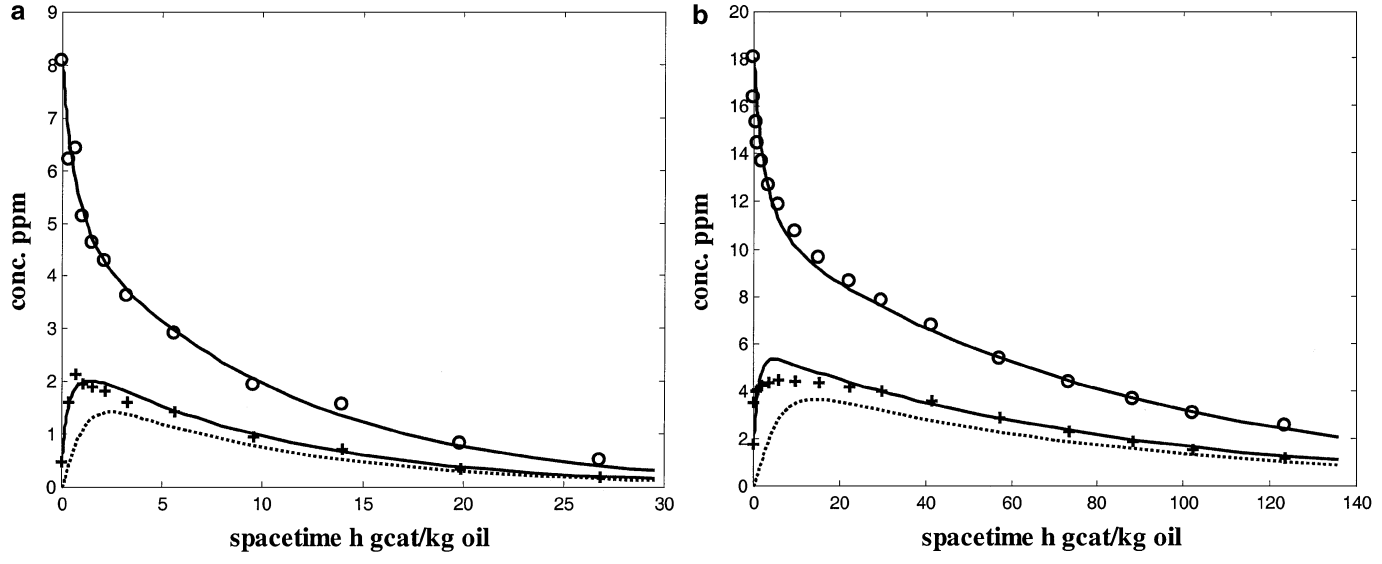

FIG. 10. Typical experimental and modeling results of VO-EP HDM for Model 3 with VF8 (a) and VF16 (b). Solid lines represent the modeling results Dash lines represent the expected values of the second intermediate. Symbols: (○) concentration of VO-EP; (+) concentration of VO-EPH_2. Conditions: 5 MPa, 543 K.)

TABLE 2

Kinetic Parameters of VF8, −12, −15, and −16 Obtained from Model 3

	VF8	VF12	VF15	VF16
k_1[a] (kg oil/g cat. h)	0.8137 ± 0.1286	0.1658 ± 0.0459	0.1546 ± 0.0390	0.2375 ± 0.0533
k_2[a] (kg oil/g cat. h)	1.2816 ± 0.5781	0.5305 ± 0.5327	0.1107 ± 0.0517	0.1771 ± 0.0828
k_3[a] (kg oil/g cat. h)	0.4598 ± 0.1102	0.0920 ± 0.0302	0.0265 ± 0.0056	0.0565 ± 0.0131
s^2[b]	0.0396	0.7489	0.7203	0.3339
Catalyst wt. (g)	0.668	1.093	0.476	0.479
Initial concn (ppm)		36.912	31.177	23.5
Zero reaction time concn (ppm)	8.560	22.364	27.667	19.856
k_2/k_1	1.5750	3.1996	0.7160	0.7457
k_3/k_1	0.5651	0.5549	0.1714	0.2397

[a] The error margins are 95% confidence intervals.
[b] s^2 is the mean sum of squares of deviation between experimental and calculated concentrations.

make up for the inadequacy of Model 1. This was explained by the small adsorption constants of porphyrinic species on the catalyst (0.0084 ppm^{-1} for VO-T3MPP) (17), and low reactant concentration (the solubility limit of VO-EP in white oil is 40 ppm) (3).

2.2.2. Fitting the experimental data with a new model. On the basis of the analysis above, a new model (Model 3, Fig. 5a) in which the deduced reaction mechanism was fully considered was suggested, thereby all the observations were explained. In Model 3 when k_1 was the slowest step, the second and third steps could be lumped into one step so that Model 3 would be simplified into Model 1 just as the others had observed (3, 7). In contrast, under our experimental conditions the slowest step was k_3 instead of k_1. In the beginning of the reactions, the concentration of VO-EPH_4 was very low so the influence of the k_5 route was negligible and Model 1 fit the data well. Around the time when VO-EPH_2 reached its maximum so that VO-EPH_4 concentration had built up, the influence of the route k_5 could no longer be neglected, leading to obvious deviation in fitting the full-time data with Model 1 as shown in Fig. 6.

The rate expressions of Model 3 are shown in Fig. 5b. In the evaluation of the kinetic data with Model 3, the hydrogenation and dehydrogenation rate constants were not introduced as independent variables, but the ratios k_4/k_1 ($= K_{14}$) and k_5/k_2 ($=K_{25}$) were kept constant. The values found best suited to K_{14} and K_{25} for all the runs under 5 MPa of total pressure were 1.8 and 1, respectively. The typical experimental and modeling results with Model 3 are given in Fig. 10 and Table 2. Obviously the new model fit our experimental data much better than Model 1 did: it followed the concentration track of the reactants (VO-EP and VO-EPH_2) very well for most reaction time especially in the beginning period and the late quasi-equilibrium period.

The only inadequacy of Model 3 was the relatively larger deviation around the time when VO-EPH_2 reached its maximum as shown in Fig. 10. This was explained by the largest adsorption of VO-EPH_2 on the catalyst at that time. The situation at zero reaction time was characterized by almost saturated adsorption by VO-EP and negligible adsorption by VO-EPH_2 on the catalyst. With progress of the hydrogenation reaction, VO-EPH_2 concentration increased, and so did the adsorbed quantity of VO-EPH_2 on the catalyst. Therefore, the amount of VO-EP that reacted should include the quantity of VO-EPH_2 on the catalyst. Model 3 failed to explain the little amount of VO-EPH_2 adsorbed on the catalyst, leading to relatively larger deviation around the VO-EPH_2 maximum. Moreover, the rate constants of Model 3 for all HDM runs (part of the results was shown in Table 2) showed a tendency to decrease a little when the initial concentration was increased. This was a sign that the inhibition by the reactant and products was not insignificant, so the bulk rate expressions were not completely adequate to describe the kinetics of VO-EP under our experimental conditions.

As a result, a better choice for the rate expressions for our kinetic data would be the LHHW models. Unfortunately, since only two species were determined quantitatively at present, we cannot describe the HDM kinetics of VO-EP by LHHW kinetic models, because it would lead to overparameterization. Besides, before a LHHW kinetic model can be employed for our experimental data, additional experiments are needed to determine the quantity of porphyrinic species physically adsorbed on the catalyst carrier alumina, since the amount is too large to be neglected.

CONCLUSIONS

The most widely accepted kinetic model for hydrodemetallization of vanadyl etioporphyrin comprised of a reversible hydrogenated step and a lumped hydrogenolysis step (Model 1) does not fit our experimental data, because under our experimental conditions the slowest step is the terminal hydrogenolysis instead of the first

hydrogenation, so the steps after the first hydrogenation cannot be lumped into one step in modelling our experimental data. Since the tetrahydrogenated species are found in our samples, a new model with two reversible hydrogenation steps and an irreversible hydrogenolysis step (Model 3) is proposed, and fits all data sets very well. Further studies are needed to isolate and identify the proposed tetrahydrogenated species, and determine their concentrations quantitatively. After that it is appropriate to express the newly proposed reaction mechanism in Langmuir–Hinshewood–Hougen–Watson (LHHW) kinetic models.

ACKNOWLEDGMENTS

Partial funding for the present study from Karl och Annie Leons Minnesfond for vetenskaplig forskning is gratefully acknowledged.

REFERENCES

1. Tamm, P. W., Harnsberger, H. F., and Bridge, A. G., *Ind. Eng. Chem. Process Des. Dev.* **20**, 262 (1981).
2. Hung, C. W., and Wei, J., *Ind. Eng. Chem. Process Des. Dev.* **19**, 250 (1980).
3. Agrawal, R., and Wei, J., *Ind. Eng. Chem. Process Des. Dev.* **23**, 505 (1984).
4. Ware, R. A., and Wei, J., *J. Catal.* **93**, 100 (1985).
5. Webster, I. A., and Wei, J., *Prepr. Am. Chem. Soc. Div. Petroleum Chem.* **30**, 37 (1985).
6. Quann, R. J., Ware, R. A., Hung, C. H., and Wei, J., *Adv. Chem. Eng.* **14**, 95 (1988).
7. Smith, B. J., and Wei, J., *J. Catal.* **132**, 1 (1991).
8. Rankel, L. A., *Prepr. Am. Chem. Soc. Div. Petroleum Chem.* **26**(3), 689 (1981).
9. Rankel, L. A., and Rollmann, L. D., *Fuel* **62**(1), 44 (1983).
10. Kameyama, H., Sugishima, M., Yamada, M., and Amano, A., *Sekiyu Gakkaishi* **24**, 317 (1981).
11. Kameyama, H., and Amano, A., *Sekiyu Gakkaishi* **25**, 118 (1982).
12. Kameyama, H., Shibuya, M., Teshigahara, I., and Amano, A., *Sekiyu Gakkaishi* **28**, 83 (1985).
13. Weitkamp, J., Gerhardt, W., Rigoni, R., and Dauns, H., *Erdöl, Kohle-Erdgas-Petrochem.* **36**, 569 (1983).
14. Weitkamp, J., Gerhardt, W., and Scroll, D., *in* "Proceedings, 8th International Congress on Catalysis, Berlin, 1984," Vol. II, p. 269. Dechema, Frankfurt am Main, 1984.
15. Gerhardt, W., Ph.D. thesis, Technische Hochschule Karlsruhe, 1984.
16. Morales, A., Garcia, J. J., and Prada, R., *in* "Proceedings, 8th International Congress on Catalysis, Berlin, 1984," Vol. II, p. 341. Dechema, Frankfurt am Main, 1984.
17. Chen, H. J., and Massoth, F. E., *Ind. Eng. Chem. Res.* **27**, 1629 (1988).
18. Bonné, R. L. C., van Steenderen, P., van Langeveld, A. D., and Moulijn, J. A., *Ind. Eng. Chem. Res.* **34**, 3801 (1995).
19. Janssens, J. P., Elst, G., Schrikkema, E. G., van Langeveld, A. D., Sie, S. T., and Moulijn, J. A., *Recl. Trav. Chim. Pays-Bas* **115**, 465 (1996).
20. Baker, E. W., and Palmer, S. E., *in* "The Porphyrins" (D. Dolphin, Ed.), Vol. I, Chap. 11. Academic Press, New York, 1978.
21. Gevert, B. S., Otterstedt, J.-E., and Massoth, F. E., *Appl. Catal.* **31**, 119 (1987).
22. Scheer, H., and Inhoffen, H. H., *in* "The Porphyrins" (D. Dolphin, Ed.), Vol. II, p. 45. Academic Press, New York, 1978.
23. Loev, B., and Goodman, M. M., *in* "Progress in Separation and Purification" (E. S. Perry and C. J. Van Oss, Eds.), Vol. 3, p. 73. Wiley, New York, 1970.
24. Scheer, H., *in* "The Porphyrins" (D. Dolphin, Ed.), Vol. II, p. 1. Academic Press, New York, 1978.